

Flexible vapour sensors using single walled carbon nanotubes

Kunjal Parikh, Kyle Cattanach, Rashmi Rao, Dong-Seok Suh,
Aimei Wu, Sanjeev K. Manohar*

*Alan G. MacDiarmid Laboratories for Technical Innovation, Department of Chemistry,
The University of Texas at Dallas, Richardson, TX 75083, USA*

Received 11 October 2004; received in revised form 20 January 2005; accepted 7 February 2005
Available online 13 March 2005

Abstract

Thin, strongly adhering films of single-walled carbon nanotube bundles (SWNT) on flexible substrates such as poly(ethyleneterephthalate) (PET) were used for vapour sensing (hexane, toluene, acetone, chloroform, acetonitrile, methanol, water, etc.). These sensors are extremely easy to fabricate using the line patterning method. For example, '4-probe' sensor patterns are drawn on a computer and then printed on overhead transparency (PET) sheets. These PET patterns were coated with films of electronically conductive SWNT bundles (1–2 μm thick) by dip-coating in aqueous surfactant-supported dispersions and mounted in glass chambers equipped for vapour sensing. Experiments conducted under saturated vapour conditions in air showed sensor responses that correlated well with solvent polarity [$E_T(30)$ scale]. Similar results were obtained under controlled vapour conditions (no air) at 10,000 ppm. Control experiments using films of carbon black on PET (Aquadag-E®), also prepared by the line patterning method, showed very little response to vapours under identical experimental conditions. The sensors are very flexible, e.g., they can be bent to diameters as small as 10 mm without significantly compromising sensor function.
© 2005 Elsevier B.V. All rights reserved.

Keywords: Organic vapour sensing; Flexible sensors; SWNT sensors; Line patterning; Transparent organic circuits; All-organic sensors

1. Introduction

Using the line patterning method [1], we describe an extremely simple method to fabricate flexible plastic sensors based on conductive coatings of single walled carbon nanotube (SWNT) bundles. The application of these films for organic vapour sensing builds on our recent findings on strongly adhering conducting coatings of SWNT on poly(ethyleneterephthalate) (PET: 'overhead transparency') whose electrical and optical properties rival commercial PET-supported conductive coatings of indium tin oxide (ITO) [2].

Sensors based on monitoring resistance changes upon exposure to vapours include active materials based on metal-oxide semiconductors (MOS) [3,4], electronic organic polymers [5–7] and polymeric systems which undergo a reversible swelling upon exposure to vapours [8,9]. Those involving changes in capacitance include transistors (ChemFETs) us-

ing MOS [10] and hybrids consisting of MOS and polymers [11]. High surface area materials like carbon nanotubes have recently shown considerable promise in organic vapour sensing [12]. Both multi-walled and single-walled carbon nanotubes (MWNT, SWNT) have been used to sense a variety of gases, e.g., NO_2 [13–18], NO_2/NH_3 [15,19–21], O_2 [22,23], H_2 [24,25], DMMP [26] hydrocarbon vapours [27,28] and other common organic vapours [27]. SWNT have more recently been used as coatings to enhance the sensing properties of SAW sensors [29]. Most of the above sensor systems are based on the use of rigid substrates such as Si or ceramics. While there are a number of reports on flexible organic transistor type devices such as transistors and ChemFETs [30–33], there are very few reports that describe flexible lightweight sensors, and even these involve complicated soft-lithographic techniques [33]. To the best of our knowledge, there has not been a report describing organic vapour sensing as a function of sensor flexibility. Even among studies on vapour sensing using carbon nanotubes, only a few describe the role of bundles of SWNT as the active sensing

* Corresponding author. Tel.: +1 972 8836536; fax: +1 972 8836586.
E-mail address: sanjeev.manohar@utdallas.edu (S.K. Manohar).

agent as opposed to individual SWNT [15,27,34]. In this paper we describe the fabrication and performance characteristics of a robust and flexible vapour sensor based on films of SWNT bundles deposited directly from aqueous surfactant-supported dispersions on plastic substrates. Flexibility data is also provided demonstrating that these films can be bent significantly without loss of sensor function. It is to be pointed out that this study is primarily an attempt to demonstrate the generality of the phenomenon of organic vapour sensing using carbon nanotubes coated on flexible plastic substrates and to ascertain if any structure/function properties can be gleaned from the data. It is not an attempt to evaluate sensor function at low vapour concentrations. This is primarily due to our choice of the line patterning method to fabricate our sensor patterns. One of the advantages of the line patterning method is that it involves no printing techniques or lithography, i.e., only traditional office equipment (computer, laser printer, overhead transparency, etc.) is necessary. These advantages are counterbalanced by limitations in the resolution of the active sensor area (70 μm) necessitating relatively large concentrations. We defer our sensor studies at low vapour concentrations (ppm levels) to subsequent reports.

2. Experimental

2.1. Materials

All powder samples of SWNT bundles were purchased from Carbon Nanotechnologies Inc., viz. (i) 'as-synthesized' by the high-pressure carbon monoxide process (as-synthesized HiPco-SWNT), (ii) HiPco-SWNT that had been chemically purified (purified HiPco-SWNT) and (iii) graphite paste purchased from Ladd research (Aquadag-E[®] # 60785). Aqueous surfactant-supported dispersions of SWNT bundles were prepared using the general procedure described in the next section. All organic solvents used were purchased (HPLC grade) from Sigma–Aldrich. Polyoxyethylene (10) isoctylphenyl ether [Triton-X 100 (TX100)], was purchased from Sigma–Aldrich and *D*, α -tocopheryl polyethylene glycol 1000 succinate, [Vitamin E TPGS (VE-TPGS)], was purchased from Eastman Chemicals. Poly(ethyleneterephthalate) (PET: 'overhead transparency') was purchased from Yamanashi University (Japan), adhesive tape from Office Max and 2 L glass jar from VWR.

2.2. Carbon nanotube dispersions

To a continuously bath-sonicated aqueous 0.6 wt.% solution of TX100 (or VE-TPGS) in 20 mL, was added, 0.16 wt.% SWNT powder. After 10 min, the dark-black dispersion was ultra-sonicated for 35 min and probe-sonicated for 24 min, in 0.5 s pulses, using Sonic Dismembrator Model 500 equipped with a 0.5 in. diameter tip operating at 30 W. The resulting homogeneous meta-stable dispersion was used within 48 h for preparing substrate-supported films. Corresponding films

using carbon black (control experiments) were prepared using an aqueous dispersion of carbon black made by diluting commercial Aquadag-E[®] paste with de-ionized water at a paste:water ratio of 1:4.

2.3. Instruments

A Keithley model 2000 digital multimeter equipped with 2000-SCAN 20-pole switch was used for all the measurements. A model 8891 sonicator (Cole Palmer) was used for bath sonication to remove the toner lines. Probe sonication was done using a Sonic Dismembrator Model 500. Scanning electron microscopy (SEM) was performed using LEO model 1530VP Field Emission SEM (Leo) and an optical microscope using reflecting mode was used for measuring film thickness. Elemental analyses was performed by Galbraith Laboratories. Electrical contacts on the sensor were made using SIP socket # 66F8665 purchased from Newark Inone.

2.4. Sensor fabrication using line patterning

The overall features of the line patterning method has been described elsewhere [1]. On a computer screen a black and white pattern representing the sensor was first drawn using standard DesignCAD-2000 software. Multiple images may be drawn on a screen. Each image consists of five lines of which four outer lines taper down to a narrow rectangular region representing the 'active sensor area' (centre line is not used in this study). The black and white colours were then inverted on the computer screen with the drawings now appearing white and the screen black. This inverted image was printed on an overhead transparency sheet using standard office laser printer. Individual images were then cut and used for dip coating into dispersions of SWNT bundles (described above). The back-side of the PET was masked by adhesive tape. The dip-coating procedure typically consists of: (i) immersing the PET/image in the SWNT dispersion for 15 s and removing it from the dispersion, (ii) after 20 s, repeating the process three more times (total four immersions). A light-brown-grey coating is seen in the image after four immersions for purified HiPco dispersions. The number of iterations is, expectedly, dependent on the properties of the dispersion used, e.g., SWNT, surfactant type, sonication time, etc. After room temperature drying for 10 min, the SWNT-coated PET/image was bath sonicated in toluene for 8–12 s which removes the 'background' toner lines cleanly leaving only the conductive coating of SWNT on the PET (Fig. 1a). Film thickness was typically 1–2 μm (SEM, optical microscopy) (Fig. 2a).

2.5. Electrical measurements

The circuit diagram used to continuously monitor changes in the 4-probe resistance of the sensor as a function of exposure to organic vapours is shown in Fig. 1b. Current is passed between the outer leads and voltage is measured between the

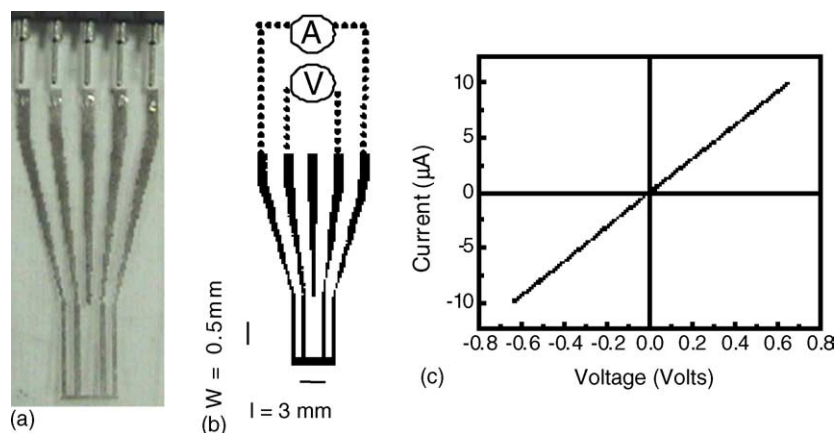


Fig. 1. (a) Optical image of an actual SWNT/PET sensor, (b) schematic of sensor circuit connections, and (c) four-probe I - V plot of purified HiPco SWNT/PET sensor.

inner leads. Our sensors show linear I - V characteristics for current values between -10 and $+10 \mu\text{A}$ (Fig. 1c). It is to be noted that the active sensor area comprises both the rectangular section and the ‘four leads’ since they are both composed of a film of SWNT bundles. We have also fabricated analogous sensor patterns in which only the rectangular part is composed on SWNT while the part comprising the four leads is composed of Pt, Au, etc. While both types of sensors can be successfully used for organic vapour sensing, reliable, consistent results were obtained when both the bottom rectangular part and the ‘four leads’ were composed of SWNT. Electrical contacts were made to the flexible sensors by soldering a platinum wire to an SIP socket attached to the carbon nanotubes of the sensors. A Keithley 2000 digital multimeter was employed to continuously monitor changes in the resistance values during exposure to organic vapours. Lab-View 6.0 interfacing software was used to monitor resistance changes of five sensors simultaneously. All experiments were conducted at room temperature. Flexibility experiments were performed by bending the overhead transparency by varying degrees while continuously monitoring the sensor response as a function of exposure to organic vapour. Bent sensor samples were held in place during the experiment by making simple modifications to the lid of the glass jar. The bending angle was measured using a goniometer, from which the extent of

bending was calculated in terms of diameter, i.e., smaller the diameter, the larger the bending angle.

2.6. Organic vapour sensing

The experimental setup is extremely simple and consists of a 2 L glass chamber with a Teflon[®] taped plastic lid with outlets for a vacuum pump and for a syringe to introduce organic solvents used in vapour sensing. To the bottom of the lid are attached five SWNT/PET sensors configured for five independent 4-probe sensor measurements simultaneously for a given organic vapour. In a typical experiment, for example, these five sensors would be films composed of: (i) ‘as-synthesized’ HiPco SWNT obtained from dispersions made from TX100, (ii) ‘as-synthesized’ HiPco SWNT obtained from dispersions made from VE-TPGS, (iii) purified HiPco SWNT obtained from dispersions made from TX100, (iv) purified HiPco SWNT obtained from dispersions made from VE-TPGS, (v) carbon black (Aquadag-E[®]) used as the control.

For vapour sensing under saturated vapour conditions, 10 mL of the organic solvent under study is injected via syringe into the glass jar and allowed to reach equilibrium with the (saturated) vapour above it (20 min). After continuously monitoring changes in the resistance for a given period of

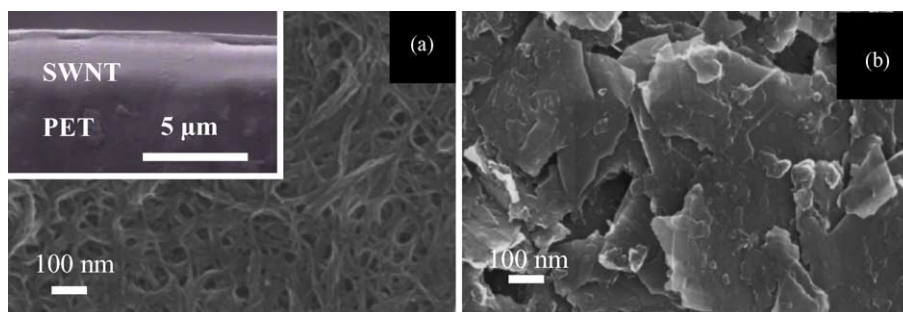


Fig. 2. SEM images of (a) SWNT/PET film (inset: cross-section), and (b) carbon black/PET film.

time, the bottom glass chamber was lowered exposing the sensor part to ambient laboratory air. Resistance changes, now under laboratory air was also continuously monitored during this time. This constituted one full cycle. For the second cycle, the glass jar was raised to its original position and resistance changes measured in a manner analogous to the first cycle. In a typical cycle the sensor was exposed to saturated vapour for 5 min followed by exposure to air for 5 min. The change in resistance measurements upon exposure to organic vapour was measured in terms of $\Delta R/R$ for a specified time period (see Section 3). A total of 28 vapours were tested under saturated vapour conditions.

For vapour sensing at 10,000 ppm, the glass jar was first evacuated using a vacuum pump followed by establishing a static vacuum. Organic solvent corresponding to an amount of 10,000 ppm (using ideal gas conditions) was injected via syringe into the glass jar. Under vigorous magnetic stirring, all of the injected liquid was converted to vapour. After 10 min, the stirring was stopped and resistance changes measured continuously with time. After a given time period, the vapour was pumped out of the glass chamber and resistance changes measured once again. This constituted one cycle. There was a 10 min break between cycles. For a typical vapour, four cycles were run with resistance measurements being recorded between the second and vapours were tested at 10,000 ppm.

3. Results and discussion

The SEM image of SWNT/PET film (Fig. 2a) shows a densely packed mat of nanotube bundles having an average diameter in 20–40 nm range and a thickness of 1–2 μm (Fig. 2a, inset). For comparison the SEM image of analogously synthesized carbon black/PET film is shown in Fig. 2b. The elemental composition described in Table 1 shows that ‘purified’ HiPco samples contain less Fe, but a significant amount of oxygen. This suggests that the harsh oxidizing acids that are used to reduce Fe levels during the purification step, also introduce oxygen in the sample, presumably in the form of carboxy and/or hydroxyl groups along the outer walls of the SWNT bundles and/or at the edges. Best sensor results in terms of ease of fabrication and robustness of response to organic vapours were obtained using the ‘purified’ HiPco SWNT samples suggesting that chemically bound oxygen could be important to overall sensor performance. This could be related simply to better adhesion between PET and SWNT bundles in oxygen-rich samples rather than to any intrinsic properties in ‘as-synthesized’ SWNT samples. In addition, the surfactant used for preparing the SWNT dispersion plays

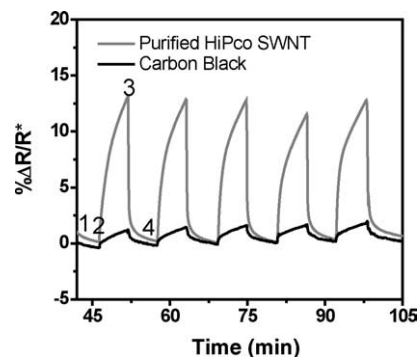


Fig. 3. Sensor response of SWNT/PET (grey) and carbon black/PET (black) films upon exposure to saturated toluene vapour. * Denotes $\% \Delta R/R$ for 5 min exposure to saturated vapour.

an important role in device fabrication, e.g., films prepared using dispersions made from non-ionic surfactants (TX100, VE-TPGS), are more uniform and strongly adhering compared to analogous films made using anionic surfactants like sodium dodecylbenzenesulfonate (SDS). It is also important to note that FT-IR spectra on analogous SWNT films on AgCl substrate before and after sonication in toluene show that residual surfactant is readily removed during sonication. Should these results translate to PET substrates, the strong adhesion of SWNT bundles to the PET substrates and the observed sensor response may not be related to residual, but rather to properties intrinsic to SWNT bundles.

Fig. 3 shows the electrical response (in $\Delta R/R$ per unit time) of SWNT/PET and carbon black/PET coatings to saturated toluene vapour under ambient conditions. The $\Delta R/R$ values are for a specified time interval and, are therefore not absolute values. After an initial steady resistance value is reached under ambient conditions (point 1), the sensor pattern was exposed to saturated toluene vapour (point 2). After 5 min, the sensor was exposed to laboratory air (point 3) by removing the glass jar containing toluene (see Section 2). After 10 min, the sensor was exposed to toluene vapour once again (point 4), and the cycle was repeated several times. The SWNT/PET coatings show a significantly enhanced response compared to carbon black in spite of both having large available surface areas, e.g., SWNT/PET coatings shows >400% change in response (14%) upon exposure to toluene compared to carbon black (3%).

As we reported in our earlier work SWNT/PET films remain conducting even when bent to a crease [2]. We carried out organic vapour sensing as a function of bending diameter to values as low as 10 mm. At each bending angle, the sensor was exposed to acetone under saturated conditions for 2 min and exposed to lab air for 5 min. The above cycles were

Table 1
Elemental analyses of SWNT powders used in this study

Sample	C (%)	H (%)	N (%)	O (%)	Fe (%)	Total (%)
Purified HiPco	83.22	1.39	<0.5	5.15	6.88	97.14
As-synthesized HiPco	61.05	–	–	–	37.98	99.03

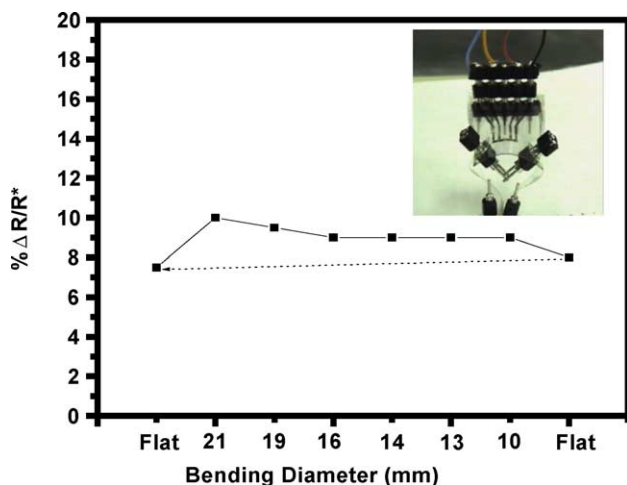


Fig. 4. Plot of sensor response as a function of device flexibility. * Denotes % $\Delta R/R$ for 5 min exposure to saturated vapour.

repeated at least five times. As one can observe from Fig. 4, there is <5% change in 4-probe resistance between the two extreme (flat) measurements, i.e., before and after a series of resistance measurements were made at progressively increasing bending degrees (decreasing diameter). The above results indicate that even under an applied stress, the SWNT film maintains its integrity and sensor function. It is not clear at the present time why electrical connection is not broken even when the SWNT/PET is bent to a crease. Although the SEM image of the SWNT/PET film shows a preponderance of 20 nm bundles, we cannot rule out contributions to electrical conductivity and hence sensor function from much smaller diameter individual tubes that could be uniformly distributed around these bundles and/or could form a layer between the bundles and the PET surface. It is possible that an underlayer of individual nanotubes could help retain sufficient electrical connection when the film is being bent. Indeed, the extensive probe sonication steps used in preparing surfactant supported SWNT dispersions might be expected to cause at least some degree of debundling. It is possible that this could also be responsible in part for the unusually strong adhesion of the SWNT film to the PET surface.

Twenty-eight organic solvents scanning a wide polarity range were evaluated under saturated vapour conditions. Compared to carbon black, SWNT/PET coatings show large, reproducible responses to a variety of vapours ranging in polarity, molecular weight and vapour pressure. Robustness in sensor function includes not only reproducibility over multiple cycles but also to sensor response to a given vapour after the sensor has been used several times to sense a variety of other organic vapours, as has been observed in the case of carbon black filled polyurethane vapour sensors [35]. For example, the sensor response to toluene vapour was $\Delta R/R = 14$ the first time and 11 after the sensor was used to measure nine other vapours (Fig. 3). This result is surprising since repeated exposure to harsh organic vapours under saturated conditions in laboratory air might be expected to severely

stress the system, e.g., to swell the PET substrate and change the dimensions of SWNT by physisorption or chemisorption, loosen the adhesion of the SWNT film to the PET substrate, etc. For example, films of carbon black do not maintain their robust response after repeated exposure to organic vapours.

It is to be noted, however, after three full cycles of twelve different organic vapours (four cycles/vapour), there is a general decline in overall sensor response and reproducibility. This could be due to PET substrate and not to the SWNT film, e.g., organic vapours such as chloroform, toluene, etc., have been reported to swell PET, and repeated exposure to these vapours could have loosened the adhesion of the SWNT film to the PET surface or metal connection at the top of the glass vessel. Vapours like DMF, DMSO, etc., cause irreversible changes in sensor response, which is consistent with their ability not only to swell plastics, but to also form strong associations with SWNT [36,37] (and hence to loosen the adhesion of the SWNT film to the PET surface).

Fig. 5 describes the sensor response as a function of concentration for a typical polar vapour (acetone) and a non-polar vapour (hexane). A general linear response is observed with increasing vapour concentration with a significantly greater response for acetone as has been observed in the case of NO_2 [15]. This suggests that solvent polarity is important in vapour/SWNT interactions (see following section).

While results obtained under ‘stressed’ saturated vapour conditions in air can help highlight the generality of the phenomenon of organic vapour sensing using flexible SWNT/PET films under ambient conditions, very little quantitative structure-function information can be extracted from the data in view of potential interference from oxygen, water vapour, etc. In addition, under saturated vapour conditions the concentrations of vapours are different for different vapours given the differences in saturated vapour pressure. Organic vapour sensing was therefore conducted at a controlled vapour concentration of 10,000 ppm. This level was chosen because of the diversity of vapours that show response under these conditions and the ease with which the vapour can be introduced via syringe in our simple experimental setup. At levels lower than 5000 ppm the results were not very reproducible given the large sensor area (see Section 1).

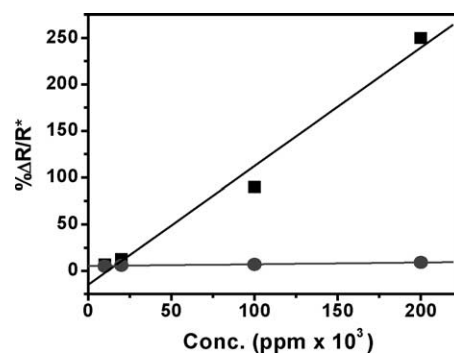


Fig. 5. Plot of sensor response as a function of vapour concentration: acetone (■) and hexane (●) % $\Delta R/R$ for 20 min exposure to vapour.

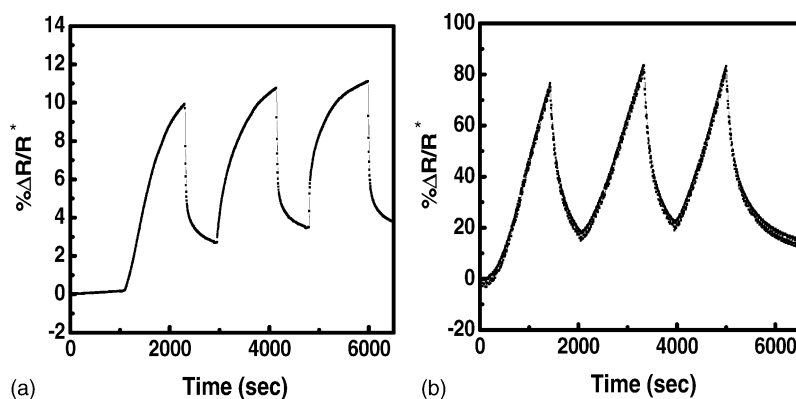


Fig. 6. Sensor response of SWNT/PET upon exposure to vapour at 10,000 ppm, (a) toluene, and (b) water. * Denotes % $\Delta R/R$ for 20 min exposure to vapour.

Results obtained from testing under single-vapour conditions at 10,000 ppm show that the trends observed under saturated vapour conditions (air/humidity) are maintained at 10,000 ppm (no air/humidity). Fig. 6 shows change in electrical response (in $\Delta R/R$) versus time plots of two representative vapours (9 tested). Thereby, conductivity of the SWNT/PET sensor changes, e.g., changes from 0.36 to 0.21 S/cm upon exposure to water at 10,000 ppm. This suggests that vapour/nanotube interactions are key to sensor function and response, as reported in vapour sensing using O_2 , NO_2 , NH_3 [14,15,17].

The precise mechanisms associated with organic vapour sensing with SWNT/PET coatings are unclear and while it is tempting to focus entirely on vapour/SWNT interactions, we cannot rule out contributions from vapour sorption by the PET substrate. For example, any swelling of the PET substrate upon exposure to vapour is expected to increase inter-bundle distance in the SWNT film, and hence, its resistance. It is to be noted, however, the low sensor response in the case of carbon black/PET films suggests that swelling of the PET film is unlikely to be a major contributor. In addition, given the high sensor response to water vapour, we cannot rule out contributions from inadvertent water in the experiments carried out at 10,000 ppm, although the overall reproducibility of sensor response both within a single run of nine vapours and between consecutive runs suggest that it is not playing a significant role.

Quantitative attempts at structure/function correlation between vapour/tube molecular interactions and sensor response [14,15,17], is thwarted by large film thicknesses, high vapour concentrations (non-ideal behaviour), and potential vapour sorption by the PET substrate. We believe, therefore, that our sensor design and architecture do not readily lend themselves to thermodynamic analysis like the linear solvation energy relationships (LSER) models that have been successfully used in polymer-coated surface acoustic wave sensors [38]. Qualitative, empirical structure/function correlations should, however, be possible in view of the unusually robust reversible sorption–desorption cycles over a wide array of vapour types.

Interaction of vapours with SWNT could either be ‘general’ or ‘specific’ with non-directional, electrostatic and dispersion forces characterizing ‘general’ interactions and directional effects like H-bonding, charge transfer, etc., characterizing ‘specific’ interactions. The experimental data suggests that vapour/tube interactions are of the ‘general’ type in which vapour sorption is largely entropy-driven. Sensor response is higher for vapours containing lone pair of electrons and/or aromatic π -electrons suggesting that dipolar electrostatic forces are important [28]. The very low response observed in the case of linear, non-polar alkanes suggests that vapour polarizability is key to sensor function, i.e., simple non-polar/non-polar effects are not sufficient. Both physisorption and chemisorption are possible in our system although the large inter-bundle distances in the SWNT film and the low redox properties of the vapours used point to a highly reversible intra-bundle physisorption mechanism. In our experiments, the resistance always increases upon exposure of the SWNT film to vapours regardless of vapour type, pointing once again to a reversible ‘general’ physisorption process which is to be contrasted with published work where vapour/tube interactions are driven largely by ‘specific’ charge-transfer effects, e.g., the NO_2 /SWNT system, where the resistance decreases upon exposure to NO_2 vapour [15].

Despite the challenges to quantitative structure/function analyses, we believe it should be possible to evaluate the overall sensor response against a wide array of solvent (vapour) parameters and polarity scales. It is important to note that no attempt is made at the present time to address any potential contribution to the sensor response from pure vapour/PET interactions (substrate swelling). Since different solvent parameters stress different structural or electronic vectors, any observed correlation is likely to provide important insights into vapour/tube interactions which could then be leveraged to advantage. While there are several reports on the various mechanisms associated with vapour–tube interactions [13–15,17,28], these have featured either reactive vapours such as NO_2 , NH_3 , etc., where strong charge transfer effects are expected, or on structurally similar homologous vapours,

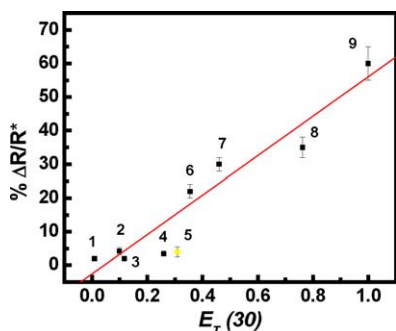


Fig. 7. Correlation plot of sensor response with solvent polarity [$E_T(30)$] scale. * Denotes % $\Delta R/R$ for 20 min exposure to vapour at 10,000 ppm.

having a limited polarity range, e.g., all hydrocarbon vapours [28]. To the best of our knowledge, we are not aware of sensor studies on SWNT films using a large variety of unreactive vapours spanning a wide polarity range.

A variety of solvent and/or vapour polarity scales were screened for possible correlation with sensor response, e.g., ‘model independent scales’ like relative permittivity, ϵ_r , modulus of the molecular dipole moment, μ , refractive index, n , Hildebrand’s solubility parameter, δ_H , and ‘model dependent scales’ based on the similarity principle like H-bonding basicity, β , the dipolarity-polarizability scale, π^* , and the Reichardt’s solvatochromic parameter scale, $E_T(30)$ [39]. We could not detect any reproducible correlation with solvent dielectric constant, dipole moment, refractive index or the α and β scales. We did, however, find a correlation with the $E_T(30)$ solvatochromic parameter scale as shown in Fig. 7. Table 2 shows the change in the resistance and $E_T(30)$ for each of the vapours tested. It is to be noted that the correlation was moderate at best, but generally reproducible over different samples and vapour concentrations. This is not surprising given the variation between sensor samples caused by differences in the fabrication process. While only nine vapours were tested at 10,000 ppm, they span a wide range of $E_T(30)$ polarity values, e.g., from 0.009 for hexane to 1.0 for water [39].

Data interpretation is further complicated by the $\Delta R/R$ values that are normalized per unit time, i.e., the values reflect a kinetic response, e.g., sensor response to a given vapour

Table 2
List of vapours tested with corresponding change in resistance and solvent polarity [$E_T(30)$]

Number	Vapour	$\Delta R/R^a$	$E_T(30)$
1	Hexane	2 ± 0.9	0.009
2	Toluene	4.25 ± 1.7	0.099
3	Ether	2 ± 1	0.117
4	Chloroform	3.5 ± 0.4	0.254
5	Dichloromethane	4 ± 1	0.309
6	Acetone	22 ± 2.4	0.355
7	Acetonitrile	30 ± 1.9	0.460
8	Methanol	35 ± 1.8	0.762
9	Water	60 ± 5	1.00

^a % $\Delta R/R$ for 20 min exposure to vapour at 10,000 ppm.

within a specified time period (efficiency). This is to be contrasted with thermodynamic effects where resistance values are measured at equilibrium (effectiveness). In essence, while the $\Delta R/R$ values obtained in this study can be viewed merely as a measure of time (not absolute), the observed correlation with the $E_T(30)$ polarity scale points to meaningful, albeit empirical tube/vapour structure-function effects.

The $E_T(30)$ scale of solvent polarity is derived from changes in the λ_{\max} of the lowest energy charge-transfer peak in the electronic spectrum of a highly aromatic zwitterionic betaine dye, pyridinium-*N*-phenolate betaine, in a given solvent [39]. The correlation of sensor response with this specific solvatochromic $E_T(30)$ scale suggests that electronic processes governing vapour/tube interactions could be qualitatively similar to those that lead to charge stabilization (solvation) of the betaine dye associated with the $E_T(30)$ scale. Although the SWNT film is not zwitterionic per se, both bulk and surface charges are expected to be present that could provide sites for interaction with organic vapours. For example, the correlation with $E_T(30)$ values observed in the case of the oxygen-rich purified-HiPco films do not translate to analogous films made from ‘as-synthesized’. In addition, the SWNT film is weakly *p*-doped with molecular oxygen playing a role in the doping process. The observed sensor response could also be due to displacement of adsorbed oxygen by the organic vapour, very much analogous to the small but significant reduction in the bulk conductivity of doped electronic organic polymers like polyaniline, polypyrrole, etc., upon removal of adsorbed H-bonding vapours like water, alcohols, etc. [40].

While interactions between the nanotube and the gas molecules are generally weak [27], a change in resistance upon exposure to vapour is believed to be due to a change in work function of the tube caused by vapour-tube dipole-dipole or charge transfer interactions. The correlation with the $E_T(30)$ scale suggest that vapour-tube dipolar effects could be playing an important role in sensor response. Computer modelling of tube-vapour interactions have shown no substantial electron density overlap between the vapour and the tube, indicating the no chemical bond is formed. It has been suggested, however, that the molecular adsorption can induce a local charge fluctuation in the region near the nanotube [27]. It has also been demonstrated that vapour adsorption can change the dielectric constant and electrical properties of SWNT [41]. These phenomena may help explain the genesis of the weak, albeit significant correlation observed with the $E_T(30)$ scale.

4. Summary

We have described for the first time: (i) organic vapour sensing using films of SWNT bundles on lightweight, transparent, plastic substrates, (ii) robust and reproducible sensor responses to a wide variety of vapours under stressed, saturated vapour conditions and under controlled vapour

conditions, (iii) a directional correlation of sensor response to the $E_T(30)$ solvent polarity scale and its potential implications to vapour/tube effects, and (iv) robust sensor response as a function of device flexibility.

The ease of device fabrication is underscored by the use of the line patterning method which permits a large array of SWNT/PET samples to be assembled in less than 1 h. It is therefore possible to rapidly screen a variety of new sensor and vapour combinations before employing more sophisticated printing or lithographic methods. Indeed, the latter may be employed after an initial screen is conducted using the approach described in this work. It is to be noted, however, that significantly more studies are needed to fully understand the robust sensor response, the strong adhesion of SWNT to the PET substrate, and contributions, if any, from vapour/substrate effects.

Acknowledgements

We gratefully acknowledge helpful discussions with Professor Alan G. MacDiarmid and for financial support from The University of Texas at Dallas. The authors are indebted to Mr. Harsha Kolla for material assistance, and Mr. Keith Bradshaw and Mr. Tom Chaddick for valuable assistance in experimental design.

References

- [1] D. Hohnholz, A.G. MacDiarmid, Line patterning of conducting polymers: New horizons for inexpensive, disposable electronic devices, *Synth. Met.* 121 (2001) 1327–1328.
- [2] N. Saran, K. Parikh, D.S. Suh, E. Munoz, H. Kolla, S.K. Manohar, Fabrication and characterization of thin films of single-walled carbon nanotube bundles on flexible plastic substrates, *J. Am. Chem. Soc.* 126 (2004) 4462–4463.
- [3] M. Utriainen, E. Karpanoja, H. Paakkanen, Combining miniaturized ion mobility spectrometer and metal oxide gas sensor for the fast detection of toxic chemical vapors, *Sens. Actuators B* 93 (2003) 17–24.
- [4] R. Ionescu, E. Llobet, S. Al-Khalifa, J.W. Gardner, X. Vilanova, J. Brezmes, X. Correig, Response model for thermally modulated tin oxide-based microhotplate gas sensors, *Sens. Actuators B* 95 (2003) 203–211.
- [5] A. Riul, A.M. Gallardo Soto, S.V. Mello, S. Bone, D.M. Taylor, L.H.C. Mattoso, An electronic tongue using polypyrrole and polyaniline, *Synth. Met.* 132 (2003) 109–116.
- [6] J.N. Barisci, G.G. Wallace, M.K. Andrews, A.C. Partridge, P.D. Harris, Conducting polymer sensors for monitoring aromatic hydrocarbons using an electronic nose, *Sens. Actuators B* 84 (2002) 252–257.
- [7] Y. Sakurai, H.-S. Jung, T. Shimanouchi, T. Inoguchi, S. Morita, R. Kuboi, K. Natsukawa, Novel array-type gas sensors using conducting polymers, and their performance for gas identification, *Sens. Actuators B* 83 (2002) 270–275.
- [8] B.C. Sisk, N.S. Lewis, Estimation of chemical and physical characteristics of analyte vapors through analysis of the response data of arrays of polymer-carbon black composite vapor detectors, *Sens. Actuators B* 96 (2003) 268–282.
- [9] E.S. Tillman, N.S. Lewis, Mechanism of enhanced sensitivity of linear poly(ethylenimine)-carbon black composite detectors to carboxylic acid vapors, *Sens. Actuators B* 96 (2003) 329–342.
- [10] D. Xie, Y. Jiang, W. Pan, J. Jiang, Z. Wu, Y. Li, Study on bis[phthalocyaninato]praseodymium complex/silicon hybrid chemical field-effect transistor gas sensor, *Thin Solid Films* 406 (2002) 262–267.
- [11] J.A. Covington, J.W. Gardner, D. Briand, N.F. De Rooij, A polymer gate FET sensor array for detecting organic vapours, *Sens. Actuators B* 77 (2001) 155–162.
- [12] L. Dai, P. Soundarrajan, T. Kim, Sensors and sensor arrays based on conjugated polymers and carbon nanotubes, *Pure Appl. Chem.* 74 (2002) 1753–1772.
- [13] C. Cantalini, L. Valentini, L. Lozzi, I. Armentano, J.M. Kenny, S. Santucci, NO₂ gas sensitivity of carbon nanotubes obtained by plasma enhanced chemical vapor deposition, *Sens. Actuators B* 93 (2003) 333–337.
- [14] A. Goldoni, R. Larciprete, L. Petaccia, S. Lizzit, Single-wall carbon nanotube interaction with gases: sample contaminants and environmental monitoring, *J. Am. Chem. Soc.* 125 (2003) 11329–11333.
- [15] J. Li, Y. Lu, Q. Ye, M. Cinke, J. Han, M. Meyyappan, Carbon nanotube sensors for gas and organic vapor detection, *NanoLett.* 3 (2003) 929–933.
- [16] J. Kong, N.R. Franklin, C. Zhou, M.G. Chapline, S. Peng, K. Cho, H. Daitl, Nanotube molecular wires as chemical sensors, *Science* 287 (2000) 622–625.
- [17] L. Valentini, F. Mercuri, I. Armentano, C. Cantalini, S. Picozzi, L. Lozzi, S. Santucci, A. Sgamellotti, J.M. Kenny, Role of defects on the gas sensing properties of carbon nanotubes thin films: experiment and theory, *Chem. Phys. Lett.* 387 (2004) 356–361.
- [18] S. Santucci, S. Picozzi, F. Di Gregorio, L. Lozzi, C. Cantalini, L. Valentini, J.M. Kenny, B. Delley, NO₂ and CO gas adsorption on carbon nanotubes: experiment and theory, *J. Chem. Phys.* 119 (2003) 10904–10910.
- [19] S. Chopra, K. McGuire, N. Gothard, A.M. Rao, A. Pham, Selective gas detection using a carbon nanotube sensor, *Appl. Phys. Lett.* 83 (2003) 2280–2282.
- [20] P. Qi, O. Vermesh, M. Greco, A. Javey, Q. Wang, H. Dai, S. Peng, K.J. Cho, Toward large arrays of multiplex functionalized carbon nanotube sensors for highly sensitive and selective molecular detection, *NanoLett.* 3 (2003) 347–351.
- [21] H. Chang, J.D. Lee, S.M. Lee, Y.H. Lee, Adsorption of NH₃ and NO₂ molecules on carbon nanotubes, *Appl. Phys. Lett.* 79 (2001) 3863–3865.
- [22] K.G. Ong, K. Zeng, C.A. Grimes, A wireless, passive carbon nanotube-based gas sensor, *IEEE Sens. J.* 2 (2002) 82–88.
- [23] P.G. Collins, K. Bradley, M. Ishigami, A. Zettl, Extreme oxygen sensitivity of electronic properties of carbon nanotubes, *Science* 287 (2000) 1801–1804.
- [24] Y.M. Wong, W.P. Kang, J.L. Davidson, A. Wisitsora-At, K.L. Soh, A novel microelectronic gas sensor utilizing carbon nanotubes for hydrogen gas detection, *Sens. Actuators B* 93 (2003) 327–332.
- [25] J. Kong, M.G. Chapline, H. Dai, Functionalized carbon nanotubes for molecular hydrogen sensors, *Adv. Mater.* 13 (2001) 1384–1386.
- [26] J.P. Novak, E.S. Snow, E.J. Houser, D. Park, J.L. Stepnowski, R.A. McGill, Nerve agent detection using networks of single-walled carbon nanotubes, *Appl. Phys. Lett.* 83 (2003) 4026–4028.
- [27] J. Zhao, A. Buldum, J. Han, J.P. Lu, Gas molecule adsorption in carbon nanotubes and nanotube bundles, *Nanotechnology* 13 (2002) 195–200.
- [28] G.U. Sumanasekera, B.K. Pradhan, H.E. Romero, K.W. Adu, P.C. Eklund, Giant thermopower effects from molecular physisorption on carbon nanotubes, *Phys. Rev. Lett.* 89 (2002) 166801/1–166801/4.
- [29] M. Penza, F. Antolini, M.V. Antisari, Carbon nanotubes as SAW chemical sensors materials, *Sens. Actuators B* 100 (2004) 47–59.
- [30] Y. Cui, Q. Wei, H. Park, C.M. Lieber, Nanowire nanosensors for highly sensitive and selective detection of biological and chemical species, *Science* 293 (2001) 1289–1292.

- [31] J. Lu, N.J. Pinto, A.G. MacDiarmid, Apparent dependence of conductivity of a conducting polymer on an electric field in a field effect transistor configuration, *J. Appl. Phys.* 92 (2002) 6033–6038.
- [32] H.T. Ng, A. Fang, J. Li, S.F. Li, Flexible carbon nanotube membrane sensory system: a generic platform, *J. Nanosci. Nanotechnol.* (2001) 375–379.
- [33] H.T. Ng, M.L. Foo, A. Fang, J. Li, G. Xu, S. Jaenicke, L. Chan, S.F.Y. Li, Soft-lithography-mediated chemical vapor deposition of architected carbon nanotube networks on elastomeric polymer, *Langmuir* 18 (2002) 1–5.
- [34] G.U. Sumanasekera, J.L. Allen, S.L. Fang, A.L. Loper, A.M. Rao, P.C. Eklund, Electrochemical oxidation of single wall carbon nanotube bundles in sulfuric acid, *J. Phys. Chem. B* 103 (1999) 4292–4297.
- [35] J.W. Hu, S.G. Chen, M.Q. Zhang, M.W. Li, M.Z. Rong, Low carbon black filled polyurethane composite as candidate for wide spectrum gas-sensing element, *Mater. Lett.* 58 (2004) 3606–3609.
- [36] J. Liu, M.J. Casavant, M. Cox, D.A. Walters, P. Boul, W. Lu, A.J. Rimerberg, K.A. Smith, D.T. Colbert, R.E. Smalley, Controlled deposition of individual single-walled carbon nanotubes on chemically functionalized templates, *Chem. Phys. Lett.* 303 (1999) 125–129.
- [37] S. Niyogi, M.A. Hamon, D.E. Perea, C.B. Kang, B. Zhao, S.K. Pal, A.E. Wyant, M.E. Itkis, R.C. Haddon, Ultrasonic dispersions of single-walled carbon nanotubes, *J. Phys. Chem. B* 107 (2003) 8799–8804.
- [38] A. Hierlemann, E.T. Zellers, A.J. Ricco, Use of linear solvation energy relationships for modeling responses from polymer-coated acoustic-wave vapor sensors, *Anal. Chem.* 73 (2001) 3458–3466.
- [39] C. Reichardt, *Solvents, Solvent Effects in Organic Chemistry*, 2nd ed., Wiley/VCH, Germany, 1988.
- [40] P.S. Barker, J.R. Chen, N.E. Agbor, A.P. Monkman, P. Mars, M.C. Petty, Vapor recognition using organic films and artificial neural networks, *Sens. Actuators B* 17 (1994) 143–147.
- [41] M. Grujicic, G. Cao, W.N. Roy, A computational analysis of the carbon-nanotube-based resonant-circuit sensors, *Appl. Surf. Sci.* 229 (2004) 316–323.